

## Electronic Supplementary Information

### Realizing High-Brightness and Ultra-wide Color Gamut Laser-Driven Backlighting by Using Laminated Phosphor-in-Glass (PiG) Films

Le Wang,<sup>\*a</sup> Ran Wei,<sup>a</sup> Peng Zheng,<sup>b</sup> Shihai You,<sup>b</sup> Tian-Liang Zhou,<sup>b</sup> Wei Yi,<sup>c</sup> Takashi Takeda,<sup>d</sup> Naoto Hirosaki,<sup>d</sup> and Rong-Jun Xie<sup>\*b</sup>

- a. College of Optical and Electronic Technology, China Jiliang University, Hangzhou, Zhejiang, 310018, P. R. China. Email: [calla@cju.edu.cn](mailto:calla@cju.edu.cn)
- b. College of Materials, Xiamen University, Xiamen 361005, P. R. China Email: [rjxie@xmu.edu.cn](mailto:rjxie@xmu.edu.cn)
- c. Nano Electronics Device Materials Group, National Institute for Materials Science (NIMS), Tsukuba, Ibaraki 305-0035, Japan
- d. Sialon Group, National Institute for Materials Science (NIMS), Tsukuba, Ibaraki 305-0035, Japan.

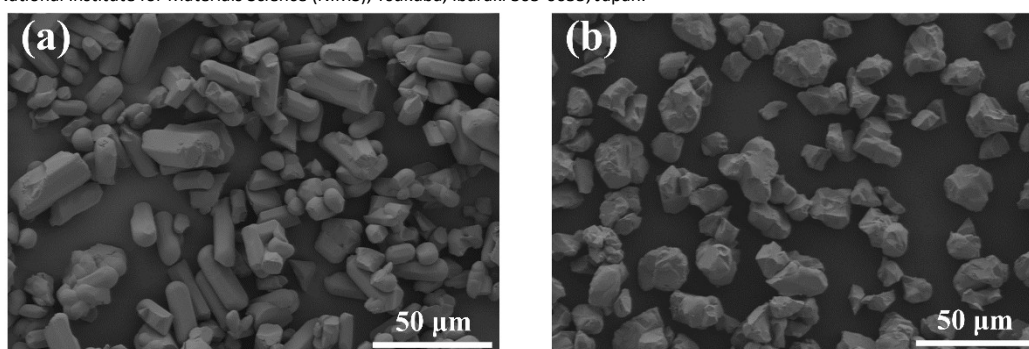


Fig. S1 SEM images of the  $\beta$ -Sialon and the Calson phosphor particles.

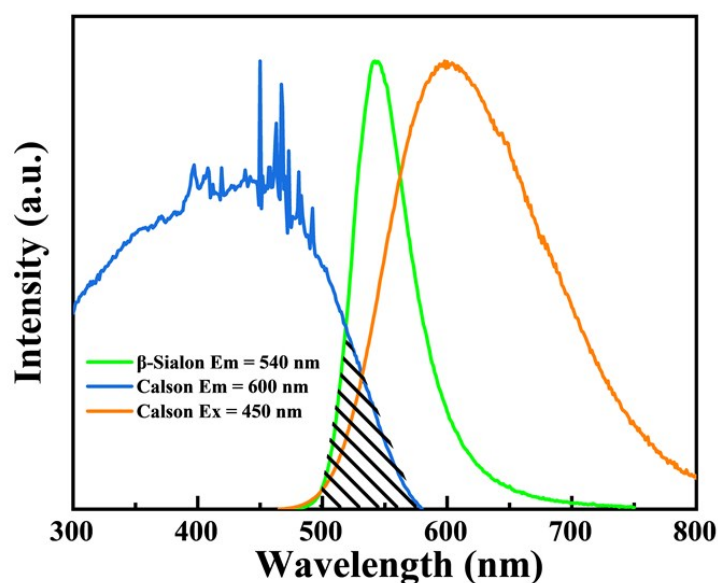


Fig. S2 Normalized PL and PLE spectra of  $\beta$ -Sialon and Calson phosphors.

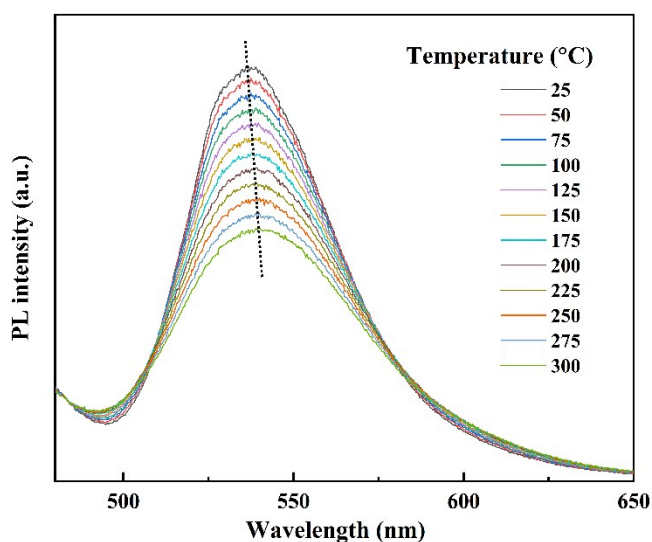


Fig. S3 Emission spectra of  $\beta$ -sialon:Eu PiG film heated at varying temperatures.

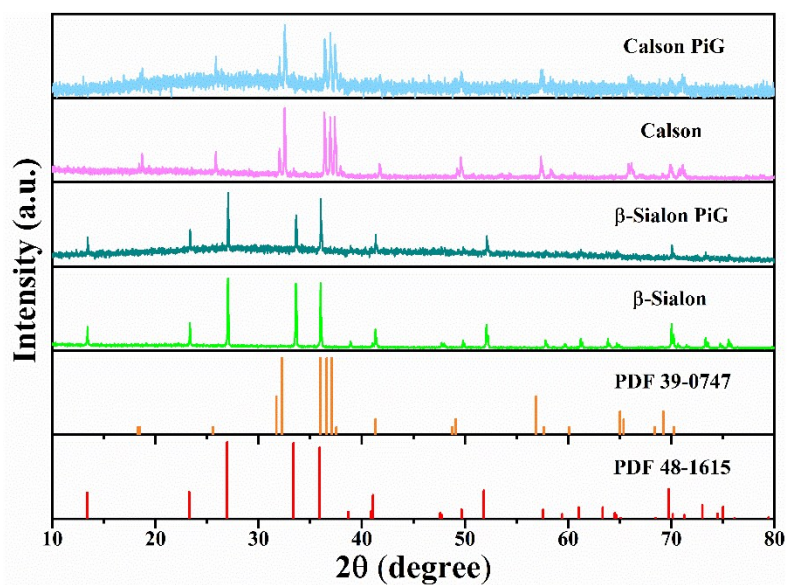


Fig. S4 XRD patterns of the phosphors, glass powder and standard patterns. PDF 39-0747, PDF 48-1615 are the standard patterns of the  $\beta$ -Sialon and the CASN.

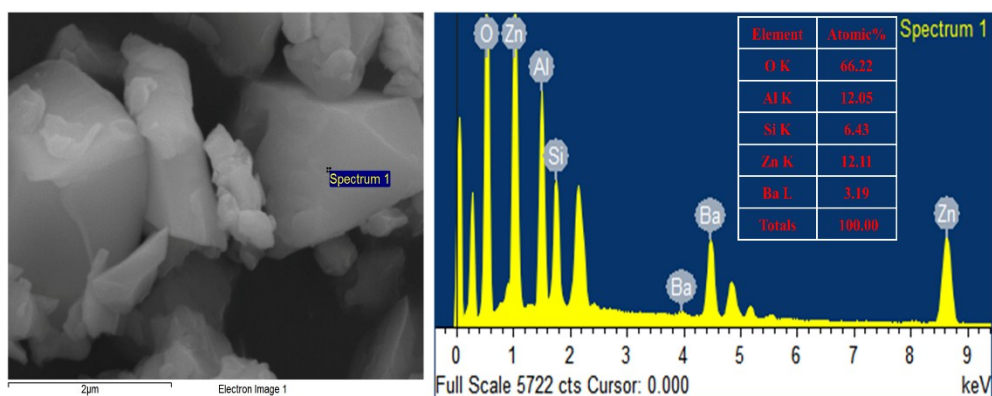


Fig. S5 The quantified elemental compositions of the glass matrix by EDS.

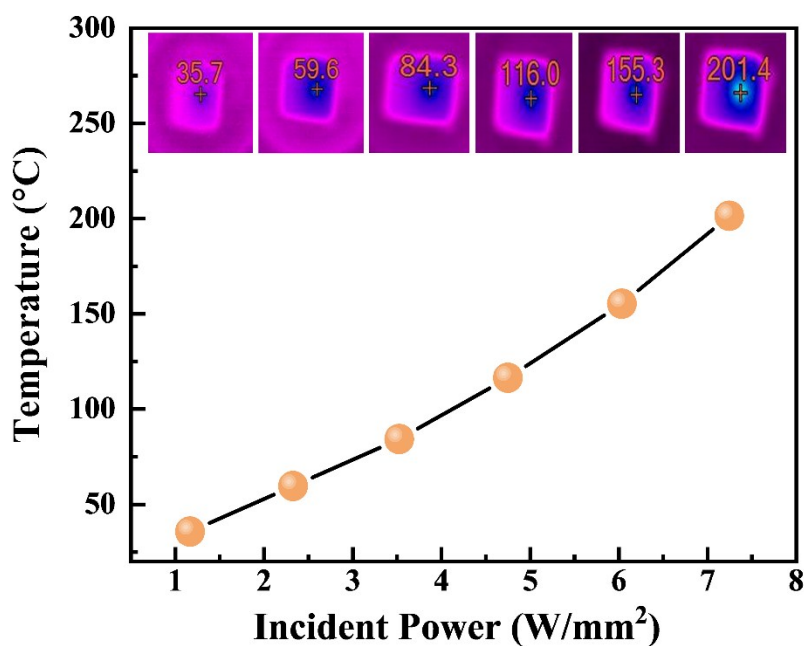


Fig. S6 The surface temperature of  $\beta$ -sialon:Eu (50 wt%) PiG film fixed at 80  $\mu\text{m}$  under the increasing laser power density.

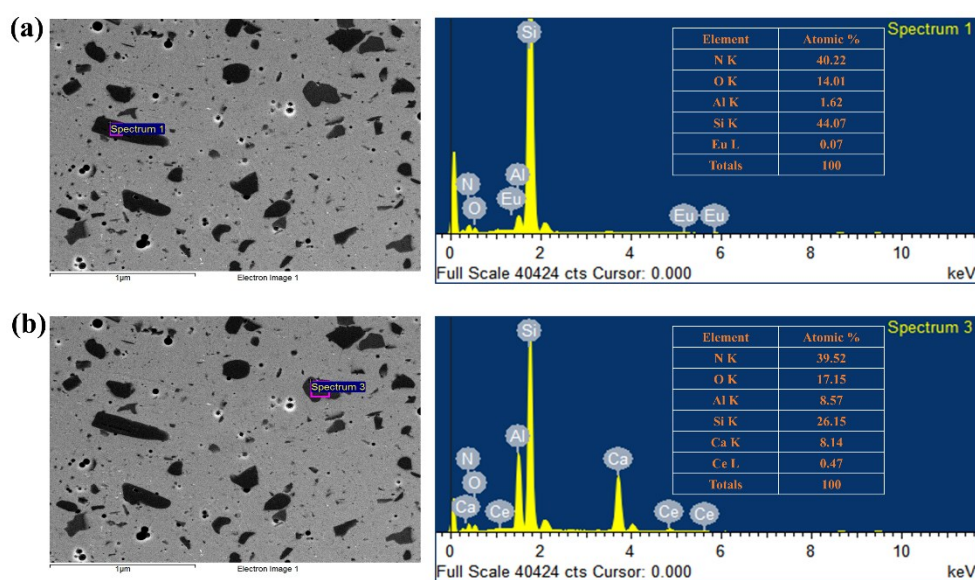


Fig. S7 The quantified elemental compositions of the G+O simple by EDS.

Tab. S1 Optical properties of the O/G ( $\lambda_{\text{em}} = 525 \text{ nm}$ ) double-layer PiG film (90  $\mu\text{m}$ ) with increasing the incident laser power.

Laser power /W	Power density /Wmm <sup>-2</sup>	Luminous flux/lm	Luminous efficacy /lmW <sup>-1</sup>	X	Y	CCT /K
0.94	1.19	41.76	44.33	0.32	0.3679	5983
1.92	2.44	81.33	42.36	0.3171	0.3542	6151
2.82	3.59	111.48	39.43	0.3137	0.342	6368
3.79	4.82	136.84	36.10	0.3086	0.3288	6733
4.79	6.09	149.82	31.27	0.3001	0.3123	7482
5.76	7.33	144.95	25.16	0.291	0.2959	8618